Journal of Advanced Ceramics
2016, **5**(3): 185–196
DOI: 10.1007/s40145-016-0189-x

ISSN 2226-4108
CN 10-1154/TQ

Research Article

Soft-chemistry synthesis of $Ba_2Ca_2Cu_3O_x$ precursor and characterization of high-T_c $Hg_{0.8}Pb_{0.2}Ba_2Ca_2Cu_3O_{8+\delta}$ superconductor

T. BRYLEWSKI[a,*], K. PRZYBYLSKI[a], A. MORAWSKI[b], D. GAJDA[c], T. CETNER[b], J. CHMIST[d]

[a]*AGH University of Science and Technology, Faculty of Materials Science and Ceramics, Al. Mickiewicza 30, 30-059 Krakow, Poland*
[b]*Institute of High Pressure Physics of the Polish Academy of Sciences, Superconductor Laboratory NL-6, ul. Prymasa Tysiąclecia 98, 00-893 Warsaw, Poland*
[c]*International Laboratory of High Magnetic Fields and Low Temperatures, ul. Gajowicka 95, 53-421 Wroclaw, Poland*
[d]*AGH University of Science and Technology, Faculty of Physics and Applied Computer Science, Al. Mickiewicza 30, 30-059 Krakow, Poland*

Received: August 18, 2015; Revised: March 22, 2016; Accepted: March 29, 2016

Abstract: The paper describes the sol–gel process applied to synthesize a mercury-free $Ba_2Ca_2Cu_3O_x$ precursor and the physicochemical properties of an $Hg_{0.8}Pb_{0.2}Ba_2Ca_2Cu_3O_{8+\delta}$ high-temperature superconductor (HTS) polycrystalline sample. The $Ba_2Ca_2Cu_3O_x$ precursor with desired chemical and phase compositions was obtained using EDTA gel process followed by decomposition and calcination under optimized conditions. An $Hg_{0.8}Pb_{0.2}Ba_2Ca_2Cu_3O_{8+\delta}$ superconductor with a fine-grained microstructure, composed predominantly of the (Hg,Pb)-1223 phase in the form of plate-like crystallites or oval grains and with advantageous magnetic properties ($T_{c(on)} = 129.2$ K, $\Delta T_c = 6.5$ K), was synthesized using the high-pressure crystallization method. At 20 K and 1 T, the critical current density of the studied sample was approximately 26 A/mm^2, while at 4 K and 1 T it increased to 155 A/mm^2. The high volume fraction of the (Hg,Pb)-1223 phase (89.1%) in the high-T_c sample was associated with the low value of the average copper valence (2.11) in the calcinated $Ba_2Ca_2Cu_3O_x$ precursor. Small amounts of non-superconducting secondary phases—$BaCuO_2$, CaO, $CaHgO_2$, CuO, Ca_2CuO, $BaPbO_3$—were also identified within the microstructure of $Hg_{0.8}Pb_{0.2}Ba_2Ca_2Cu_3O_{8+\delta}$.

Keywords: superconductor; microstructure; EDTA gel process; secondary phase

1 Introduction

The family of Hg-based high-temperature superconductors with the homologous series $HgBa_2Ca_{n-1}Cu_nO_{2n+2+\delta}$ (Hg/Ba-12(n–1)n, $n \leqslant 7$) first described in 1993 [1–4] has found wide application in the fields of power engineering and microelectronics, including new generations of devices characterized by very low energy losses, extremely rapid gates, and switches and quasitransistors based on Josephson junctions (superconducting quantum interference devices, SQUIDs). The highest reproducible transition temperatures among all cuprates, i.e., ~133 K under ambient pressure [5] and 160 K under high pressure [6],

* Corresponding author.
E-mail: brylew@agh.edu.pl

have been reported for $HgBa_2Ca_2Cu_3O_{8+\delta}$ (denoted as Hg-1223), which has only one insulating layer between superconducting blocks and therefore much better flux pinning, leading to infield critical current density (J_c) values higher than those observed for Bi-based superconducting systems [5,7]. Furthermore, the electrical and magnetic transport properties of the Hg-1223 superconductor may be modified to a large degree by partially substituting mercury with various high-valency dopants (e.g., Re, Tl, V, Se) [8–12]. Nevertheless, the fabrication of high-quality bulk samples and thick and thin films composed of mercury cuprate superconductors and deposited on appropriate substrates, with high critical T_c and J_c parameters, free from defects and resistant to environmental interactions, and thermally stable throughout the applied temperature range, remains a challenging task.

Many valuable studies presenting the syntheses of Hg-1223 superconductors and their physicochemical characteristics have been published so far [3,13–18]. The main problem faced when synthesizing these materials is that it is difficult to obtain them in the form of a single-phase bulk sample or film. This issue stems from the chemical complexity of the Hg–Ba–Ca–Cu–O system as well as the toxicity and chemical instability of HgO used as the initial reactant and its decomposition well below the temperatures necessary to crystallize the Hg-1223 phase [3]. As observed during the preparation of Bi–Sr–Ca–Cu–O and Tl–Sr–Ca–Cu–O superconductors, doping with PbO facilitates the formation of the high-T_c Hg-1223 phase in $(Hg,Pb)Ba_2Ca_2Cu_3O_{8+\delta}$ (denoted as (Hg,Pb)-1223) [19].

The typical procedure used to synthesize Hg-based superconductors comprises two basic stages: the synthesis of the mercury-free $Ba_2Ca_{n-1}Cu_nO_x$ precursor aimed at achieving the required composition of the high-temperature superconductor (HTS) phase (Hg-12(n−1)n, where $n = 1,2,3,\cdots$), and the thermal treatment of this precursor in a mercury environment, which can be carried out using high-pressure techniques [20] or the sealed quartz tube technique [21]. A review of numerous reports dealing with the methods of preparing the $HgBa_2Ca_2Cu_3O_{8+\delta}$ superconductor shows that the solid-state reaction route commonly used in the synthesis of the $Ba_2Ca_2Cu_3O_x$ precursor severely limits the ability to control the stoichiometry and makes it impossible to obtain a homogeneous superconductor with the desired phase composition [3,13–15,18].

Systematic investigations intending to explain the mechanism of the formation of the superconducting mercury phase show that—regardless of the method used to prepare the $Ba_2Ca_2Cu_3O_x$ precursor—$HgCaO_2$ and $HgBa_2CaCu_2O_{8+\delta}$ appear in the initial stage of the formation of the Hg-1223 phase. As a consequence of the intercalation of Ba–Cu–O and Ca–Cu–O, the two aforementioned phases are converted into the $HgBa_2Ca_2Cu_3O_{8+\delta}$ compound [22,23]. These investigations show that the high degree of homogenization of Ca and Cu cations in the precursor significantly affects the formation rate of the Hg-1223 phase and the rate at which its volume fraction increases in the sample [23]. As a result of the appearance of large CaO grains in the incompletely reacted $Ba_2Ca_2Cu_3O_x$ precursor, higher temperature and longer time are required to complete the synthesis [23]. The conditions in which the precursor is synthesized determine not only the composition, but also the proportion of non-stoichiometric phases to stoichiometric ones, which affects the incorporation of extra oxygen into the precursor [24]. The effect of the synthesis conditions of $Ba_2Ca_{n-1}Cu_nO_x$ precursors on their average copper valence and, consequently, on the appearance of each number n in the $HgBa_2Ca_{n-1}Cu_nO_{2n+2+\delta}$ homologous series, was investigated in Ref. [24]. This report concluded that under the same high-pressure and high-temperature synthesis conditions, higher precursor copper valence favors the formation of lower numbers n in the series, while lower precursor copper valence has the opposite effect. These experimental observations imply that in order to obtain HTS bulk samples and thick or thin films with a predominant amount of Hg-1223, it is necessary to focus on the proper selection of the conditions under which the $Ba_2Ca_2Cu_3O_x$ precursor is prepared and thermally treated [24].

Of several low-temperature chemical methods, the sol–gel methods utilizing different complexing agents such as acrylamide (AA) [21], organic (tartaric and citric) acids [25,26], or urea [18] appear to be the most promising. These methods may be used to achieve homogeneous mixtures of all components at the atomic level, yielding highly reactive powders. Moreover, these powders are not susceptible to H_2O/CO_2 contamination [23]. Taking into account the strong complexing ability of the EDTA chelating agent, a feature which facilitates the full control of stoichiometry in the cation sublattice of the $Ba_2Ca_2Cu_3O_x$ precursor [27,28], and to prevent reactions between polymeric monomers and Cu cations, which may occur when using sol–gel processing with

acrylamide [21], it is strongly recommended that EDTA gel process should be applied.

Given the slow crystallization rate and the difficulty of stabilizing the Hg-1223 phase, the thermal treatment of these materials should be carried out under high partial pressures of mercury and oxygen [3,29]. In this respect, the best effects are obtained by applying the high gas pressure method, in spite of the high cost of this solution [30,31]. When combined with sufficient knowledge in the field of the thermodynamics of the HTS phases' stability and the kinetics of their formation, this method provides conditions that allow superconducting bulk samples with single phase and fine-grained microstructure and advantageous parameters to be obtained.

The primary aim of the present paper was to synthesize a fine $Ba_2Ca_2Cu_3O_x$ precursor via the sol–gel method, using EDTA as the agent complexing the metal cations in an aqueous solution. Another goal was to thoroughly examine the physicochemical properties of the Hg-free precursor and the $Hg_{0.8}Pb_{0.2}Ba_2Ca_2Cu_3O_{8+\delta}$ superconducting bulk sample obtained using the high gas pressure method.

2 Experimental

Due to the complexity of the (Hg,Pb)$Ba_2Ca_2Cu_3O_{8+\delta}$ compound and the toxicity of the Hg-containing ingredient, the synthesis of the (Hg,Pb)-1223 bulk sample was performed in a two-step process, i.e., first preparing the $Ba_2Ca_2Cu_3O_x$ precursor and then annealing it with Hg vapor under high gas pressure conditions.

2. 1 Preparation of $Ba_2Ca_2Cu_3O_x$ precursor

The synthesis of $Ba_2Ca_2Cu_3O_x$ precursor micropowders was carried out by means of the modified sol–gel method with EDTA as the complexing agent of metal cations in an aqueous solution, also known as the EDTA gel process. The following analytical grade reagents were used as starting materials: $Ba(NO_3)_2$, $Ca(NO_3)_2{\cdot}4H_2O$, $Cu(NO_3)_2{\cdot}3H_2O$, ammonium hydroxide solution (28% NH_3 in H_2O), and EDTA (ethylenediaminetetraacetic acid). In order to purify the above reagents further, they were dissolved in twice-distilled water and crystallized. The purified salts with known dry matter content were used to prepare 0.25 M (M: molar concentration, mol/L) solutions of barium, calcium, and copper nitrates, which were subsequently mixed in the appropriate cation ratio, i.e., Ba:Ca:Cu = 2:2:3. To obtain the gel precursor, this nitrate solution was mixed with 0.1 M EDTA, the volume of which was determined from the following proportion: 1 mol of EDTA: 1 mol of metal cation. A constant pH = 7.5 was maintained via the dropwise addition of an ammonium hydroxide solution using a peristaltic pump. The aqueous solution containing the appropriate metal complexes was slowly heated and stirred at 363 K to evaporate the water until a transparent, blue, glassy gel was obtained. This gel precursor was then pyrolyzed in oxygen at 773 K for 1.5 h, ground in dry ethanol in a rotary mill for 5 h, and finally calcinated for 10 h in air at temperatures of 1073, 1113, or 1173 K.

2. 2 Synthesis of $Hg_{0.8}Pb_{0.2}Ba_2Ca_2Cu_3O_{8+\delta}$ superconducting bulk sample

The sintering and subsequent annealing of the $Hg_{0.8}Pb_{0.2}Ba_2Ca_2Cu_3O_{8+\delta}$ sample was performed by means of the high gas pressure method. The experimental high-pressure setup, reported in detail elsewhere [30–32], consisted of a 1.5 GPa gas compressor and a piston cylinder pressure chamber with an internal three-zone Kanthal furnace. The $Ba_2Ca_2Cu_3O_x$ calcinated precursor was mixed in a dry box with HgO and PbO in an amount required to obtain the initial composition of $Hg_{0.8}Pb_{0.2}Ba_2Ca_2Cu_3O_{8+\delta}$ and compacted into 10 mm pellets at 250 MPa. The pellets were then placed in a furnace setup consisting of two crucibles. The inner crucible was made of $BaZrO_3$, while the outer one consisted of Al_2O_3. The pellets were sintered at 1340±1 K for 10 min in a gas mixture with an oxygen content of 20% and under a pressure of 10 kbar, and then cooled down to 1113 K at a rate of 5 K/h. When this temperature was reached, the samples were annealed for 2 h and afterwards cooled down to room temperature at a rate of 10 K/min. Typical pressure and temperature runs applied in the synthesis of superconducting Hg-family compounds have been presented in Ref. [31].

2. 3 Analytical methods

The chemical composition of the powders was determined by means of atomic absorption spectroscopy (AAS) using the Pye Unicum SP90B spectrometer. The phase compositions of the samples

were characterized using X-ray diffraction (XRD) analysis. The volume fractions of the various phases present were determined by comparing the intensities of the strongest non-overlapping reflection from each phase. The Seifert-FPM XRD 7 diffractometer with Cu Kα radiation was used. Scanning electron microscopy (SEM, JEOL JSM-5400) coupled with energy dispersive X-ray (EDX) analysis was used to examine the morphology and chemical composition of the samples. The average copper valence of the Hg-free precursor was determined using the iodometric titration method; the details of this procedure are described in Ref. [33]. Low-temperature magnetic measurements of the superconductor were carried out with the standard mutual inductance bridge with AC magnetic field amplitude of 280 mOe and an operating frequency of 188.88 Hz. The intragranular critical current densities were estimated by measuring magnetization at 4 and 20 K using the Bean model [34]. Magnetization versus temperature (at 4 and 20 K) and magnetic field induction (up to 14 T) for the studied samples were measured using a Quantum Design PPMS Model 6000 device. The critical temperature was measured for a 10 mT magnetic field parallel to the height of the sample, which was 4 mm.

3 Results and discussion

3. 1 Gel precursor processing and decomposition

The idea of the sol–gel route applied in the present work, i.e., one based on water-soluble metal chelates, is to reduce the concentration of free metal ions in the precursor solution through the formation of strong, soluble chelate complexes which are then converted into an amorphous glassy state when the solvent is removed [28,35]. Thus, in order to avoid unwanted precipitation effects, it is necessary to apply chelating agents. The conditional stability constant β_m, which defines the relation between the complexing ion concentration of the metal and the free ions in the solution in the equilibrium state, provides a measure of the stability of these complexes [36].

For a multi-stage complexing reaction, represented by Eq. (1):

$$M + mL \Leftrightarrow ML_m \tag{1}$$

the equilibrium constant for ionic strength $I > 0$ may be defined using the expression:

$$\beta_m = \frac{[ML_m]}{[M][L]^m} = \prod_{i=1}^{m} K_i \tag{2}$$

where K_i is the *i*-th successive stability constant of the metal complexes *M* with the given *m*-number of ligands *L*, while the symbol [ ] denotes concentration. The stability of the complex in the metal–ligand system is directly proportional to the value of the β_m constant. The β_m value of the complexes containing Ba, Ca, and Cu depends on the type of the applied organic hydroxyacid. For the sake of comparison, the conditional stability constants of the complexing compounds with the respective metal cations are presented in Table 1. These organic agents are commonly utilized in chemical methods used to prepare ceramic powders via the amorphous metal–chelate route [35,36]. Since EDTA anions exhibit the highest value of the conditional stability constant β_m when chelating metal cations (Table 1), EDTA gel process may be a more effective method for the preparation of homogeneous $Ba_2Ca_2Cu_3O_x$ precursor than the sol–gel route using other chelating agents.

Table 1 Stability constants (values for log β_m and [*I*] of complexes with EDTA, citric acid, oxalic acid, and acetic acid, where β denotes the complex constant, *m* the number of ligands per complex, and [*I*] the ionic strength [35])

Metal ion	Complex			
	EDTA (hydroxyethylethylene-diaminetriacetic acid, $C_{10}H_{18}O_7N_2$)	Citric acid (2-hydroxypropane-1,2,3-tricarboxylic acid, $C_6H_8O_7$)	Oxalic acid (ethanedioic acid, $C_2H_2O_4$)	Acetic acid (ethanoic acid, $C_2H_4O_2$)
Ba^{2+}	$\log\beta_1 = 7.76$ [0.1]	$\log\beta_1 = 2.89$ [0.1]	$\log\beta_1 = 0.58$ [1.0] $\log\beta_2 = 2.20$ [1.0]	$\log\beta_1 = 0.979$ [0]
Ca^{2+}	$\log\beta_1 = 10.59$ [0.1] $\log\beta_1 = 10.45$ [0.3]	$\log\beta_1 = 3.55$ [0.1] $\log\beta_1 = 3.40$ [0.25]	$\log\beta_1 = 1.66$ [1.0] $\log\beta_2 = 2.69$ [1.0]	$\log\beta_1 = 1.12$ [0]
Cu^{2+}	$\log\beta_1 = 18.80$ [0.1]	$\log\beta_1 = 5.90$ [0.1]	$\log\beta_1 = 10.59$ [0.1] $\log\beta_2 = 9.27$ [1.0]	$\log\beta_1 = 1.89$ [0.1] $\log\beta_1 = 1.30$ [1.0] $\log\beta_2 = 2.04$ [1.0]

When determining the conditions for the synthesis of the precursor, the conditional stability constant of the complexing compounds should be considered in the context of the solution's pH [36,37], since (1) low pH results in multi-stage dissociation of metal complexes and (2) high pH causes the hydrolysis of metal ions. The concentration of the ions that complex Ba^{2+}, Ca^{2+}, and Cu^{2+} cations in the water solution is precisely determined by the solution's pH, given the competitive effect of H^+ ions which bind the ligands into hydrogenated forms, such as $HEDTA^{3-}$, H_2EDTA^{2-}, H_3EDTA^-, and H_4EDTA (Fig. 1) [35–37]. With increasing pH, the concentration of the $HEDTA^{3-}$ and $EDTA^{4-}$ ions with the strongest complexing properties increases due to the EDTA dissociation. However, a further increase in the solution's pH yields a decrease in the complexing ability of the above-mentioned EDTA ions due to the hydrolysis of metal ions, which leads to the formation of poorly soluble metal hydroxides.

The upper pH limit for specifying experimental conditions, above which no precipitation may occur during the course of concentration, may be determined from the pM'–pH diagram, where $pM' = \log_{10}([M']/(\text{mol/L}))$ [35,38]. [M'] is related to the concentration of free metal ions, [M^{z+}], through Ringbom's side-reactions coefficient, $\alpha_{M(L)}$ (L = EDTA) [37,39]:

$$[M'] = \alpha_{M(L)} \cdot [M^{z+}] \quad (3)$$

Based on the above diagram representing the borderlines of the precipitation region for various M–EDTA systems described in detail in the review paper [35], the optimal pH value for the synthesis of the Ba–Ca–Cu gel precursor was determined to be 7.5. The above-presented diagram also takes into account the possibility of the formation of insoluble $BaCO_3$ precipitates resulting from the dissolution of CO_2 originating from air in the solution.

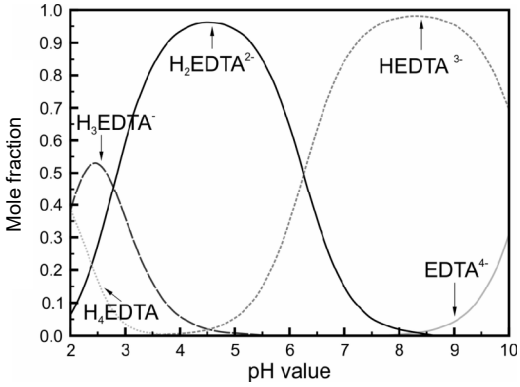

Fig. 1 pH dependence of the equilibrium distribution of various species of EDTA [34].

In a liquid precursor with pH = 7.5 adjusted via the introduction of $NH_3 \cdot H_2O$ into the mixture containing barium, calcium, and copper nitrates and the EDTA solution, the predominant ion complex is $HEDTA^{3-}$, as illustrated by the following reaction (4):

$$H_4EDTA + 3NH_3 \Leftrightarrow HEDTA^{3-} + 3NH_4^+ \quad (4)$$

The $HEDTA^{3-}$ ions formed during dissociation react with the given precursor metal cations and form stable, complex organic metal ions (Table 1):

$$\begin{cases} M = Ba^{2+}, Ca^{2+}, Cu^{2+} \\ EDTA^{3-} + M(NO_3)_2 \Leftrightarrow [M(EDTA)]^- + 2NO_3^- \end{cases} \quad (5)$$

Simultaneously, amminocopper complexes $[Cu(NH_3)_4]^{2+}$ are also formed, preventing the precipitation of copper in the form of the $Cu(OH)_2$ compound, due to the reaction (6):

$$Cu(NO_3)_2 + 4NH_3 \Leftrightarrow [Cu(NH_3)_4]^{2+} + 2NO_3^- \quad (6)$$

The dried gel precursor obtained from the starting solution under the above-mentioned conditions (pH = 7.5) exhibits mostly an amorphous structure with a minor contribution of a crystalline-like $Ba(NO_3)_2$ phase, whereas in the gels obtained for pH values equal to 6 and 9, the presence of $Cu(OH)_2$, $Cu_2(OH)_3NO_3$, and $Ba(NO_3)_2$ precipitates is observed.

According to the performed X-ray analysis, the pyrolyzed precursor obtained from the gel prepared for pH = 7.5 and subsequently decomposed in oxygen at 773 K for 1.5 h has a multi-phase composition, and contains the following phases: $BaCO_3$, CaO, CuO, Ba_3CuO_4, and $Ba(NO_3)_2$ as well as other unidentified phases. The $Ba(NO_3)_2$ phase precipitates in the form of poorly soluble barium nitrate salt during the polycondensation of the stable metal complexes in water solution. The temperature of pyrolysis was selected based on the differential thermal analysis and thermogravimetric analysis (DTA–TG), which showed that the final multi-stage decomposition of the precursor gel occurs at 723 K.

The agglomerated nature of the pyrolyzed precursor was confirmed through SEM morphological observations shown in Fig. 2. The powder grains are characterized by irregular shape and they have the ability to agglomerate due to the high surface energy of the crystallites. The mean size of these aggregates is estimated at 0.2–2 μm.

3. 2 Calcination process of $Ba_2Ca_2Cu_3O_x$ powders and characterization

Figure 3 shows the XRD patterns of the calcinated

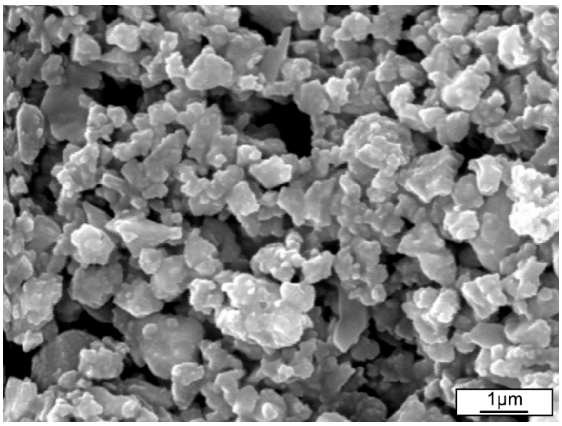

Fig. 2 SEM microphotograph of pyrolyzed precursor obtained after gel decomposition in oxygen at 773 K for 1.5 h.

$Ba_2Ca_2Cu_3O_x$ precursors obtained after thermal treatment of the pyrolyzed precursor in air for 10 h at temperatures of 1073, 1113, and 1173 K. As can be seen, after calcinating this precursor at 1073 K for 10 h, the main compounds crystallized from the previous phases are $BaCuO_2$, $Ba_2Cu_3O_5$, CaO, and CuO, while for the precursor calcinated at 1113 K for 10 h, $BaCuO_2$, Ca_2CuO_3, and traces of CuO and CaO phases are identified. Further calcination up to 1173 K for 10 h leads to the formation of only two phases—$BaCuO_2$ and Ca_2CuO_3—as shown in Fig. 3. The existence of the above phases in a well-calcinated precursor with Ba:Ca:Cu = 2:2:3 is in good agreement with the phase diagram analysis of the Ba–Ca–Cu–O system [40].

It is worth noting that in these calcination conditions, $Ba_4CaCu_3O_8$ phase is not observed; this presents a contrast to the findings of Loureiro *et al*. [24], who detected this phase when performing synthesis at higher temperatures. Thus, it may be expected that in the absence of this phase in the studied precursor, the average copper valence will be reduced, which promotes the formation of higher members n of the

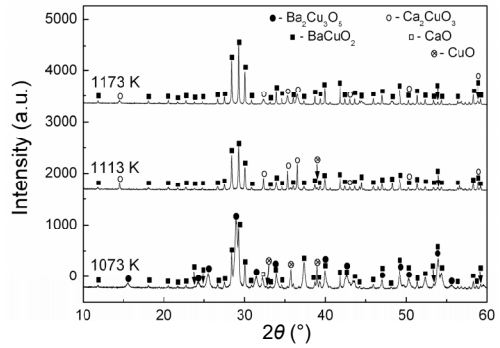

Fig. 3 XRD patterns of $Ba_2Ca_2Cu_3O_x$ precursors after calcination in air for 10 h at different temperatures.

$HgBa_2Ca_{n-1}Cu_nO_{2n+2+\delta}$ homologous series. The determined average copper valence $\langle V_{Cu} \rangle$ of the prepared $Ba_2Ca_2Cu_3O_x$ precursor is 2.11. This is supported by the data reported by Loureiro *et al*. [24], who observed contrasting results for copper valence values of 2.13(2) and 2.18(2) for the $Ba_2Ca_2Cu_3O_x$ precursor heat-treated at 1198 K for 20 h in oxygen; in the case of the lower value, they observed a single Hg-1223 phase, whereas the contribution of this superconducting phase was lower for the higher average copper valence value.

It should be noted that a properly calcinated $Ba_2Ca_2Cu_3O_x$ precursor is practically insensitive to H_2O/CO_2 contamination. During 3 months of storage in air at room temperature with a relative humidity of about 40%, this precursor gains less than 0.3% weight. AAS analysis indicated that the nominal stoichiometry of the calcinated precursor is Ba:Ca:Cu = 2.00: 2.06:2.92, which approximately corresponds to its starting composition. This proves that the precise control of stoichiometry in the cation sublattice of the $Ba_2Ca_2Cu_3O_x$ precursor may be attributed to the strong complexing ability of the EDTA chelating agent.

In order to obtain information about the shape and size of the aggregates and agglomerates of the $Ba_2Ca_2Cu_3O_x$ precursor, its microstructure was studied. The chemical composition of selected areas of the sample was also analysed using EDX. The precursor obtained as a result of calcination of the pyrolyzed precursor containing incompletely reacted oxides and carbonates is distinguished by its non-homogeneous morphology with strongly agglomerated aggregates, as shown in Fig. 4. The size of these grains varies from 1 to 5 μm. The analysis of the chemical composition of $Ba_2Ca_2Cu_3O_x$ precursor agglomerates, for instance in the area marked with symbol A (Fig. 4), reveals considerable amounts of barium and copper, which is consistent with the presence of the $BaCuO_2$ phase. Similarly, EDX analysis of the other agglomerate area—symbol B (Fig. 4)—indicates a strong accumulation of Ca and Cu due to the formation of Ca_2CuO_3.

3. 3 Microstructure and magnetic properties of $(Hg,Pb)Ba_2Ca_2Cu_3O_{8+\delta}$ superconducting bulk sample

In order to evaluate the suitability of the well-calcinated $Ba_2Ca_2Cu_3O_x$ precursor for the synthesis of $(Hg,Pb)Ba_2Ca_2Cu_3O_{8+\delta}$ polycrystalline

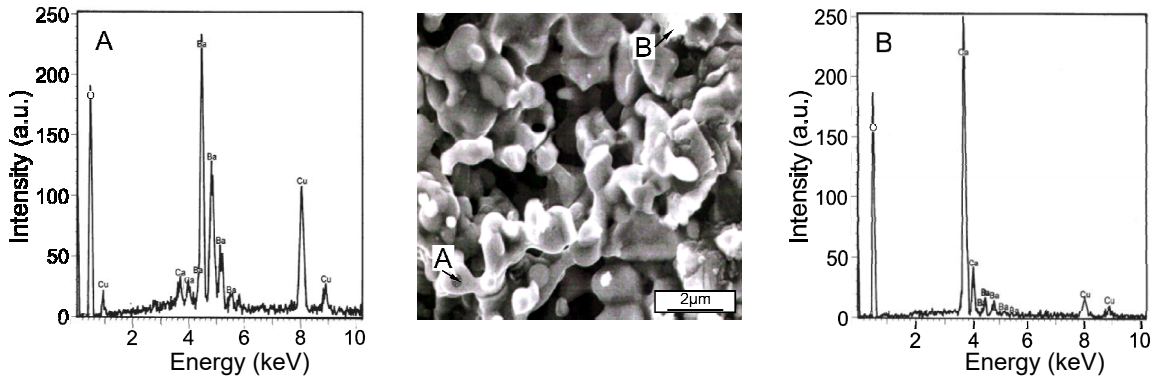

Fig. 4 SEM microphotograph of the $Ba_2Ca_2Cu_3O_x$ precursor after calcination (middle) and EDX point analysis spectra of the regions A and B marked in the microphotograph.

superconducting sample, this precursor was heat-treated in a mercury environment using the high gas pressure method, as described previously.

Figure 5 shows the X-ray diffractogram for the $Hg_{0.8}Pb_{0.2}Ba_2Ca_2Cu_3O_{8+\delta}$ bulk sample sintered at 1340 K for 10 min under high gas pressure conditions. The analysis of phase composition reveals the presence of two superconducting phases, i.e., the high-T_c (1223) and the low-T_c (1212), with most of the peaks assigned to the (Hg,Pb)-1223 phase. The refinement of the X-ray data shows that the volume fractions of the (Hg,Pb)-1223 and (Hg,Pb)-1212 phases are equal to 89.1% and 4.5%, respectively. The first of these phases, (Hg,Pb)-1223, crystallizes in an orthorhombic cell with the lattice parameters of $a = 5.426$ Å, $b = 5.421$ Å, and $c = 15.448$ Å. This crystallographic data is comparable with the previously reported values [41]. Consequently, the determined average copper valence $\langle V_{Cu} \rangle$ of the synthesized $Ba_2Ca_2Cu_3O_x$ precursor is the reason for the formation of higher numbers of the Hg-family series, i.e., (Hg,Pb)-1223 with a significant volume fraction. Additionally, the occurrence of other peaks with a total volume fraction of 6.4% is attributed to the secondary phases of $BaCuO_2$, $CaHgO_2$, $CaCu_2O_3$, and $BaPbO_3$, and CuO is also identified (Fig. 5). The most intensive peaks for the CaO phase are not observed in the diffractogram. Since CaO may hydrolyze in air to form $Ca(OH)_2$, an attempt to discover peaks of this compound was made [42]; however, none are observed. The amount of CaO, which is clearly visible via SEM in the form of very fine particles, is nonetheless too small to be detected via XRD, or appears in amorphous form.

Figure 6 shows the morphology of the $Hg_{0.8}Pb_{0.2}Ba_2Ca_2Cu_3O_{8+\delta}$ superconductor specimen sintered at 1340 K for 10 min using the high gas pressure method. The superconducting crystallites

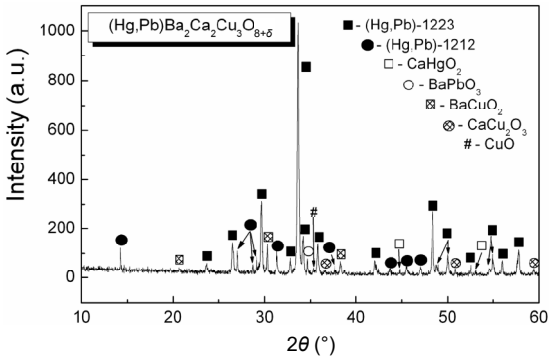

Fig. 5 XRD pattern for $Hg_{0.8}Pb_{0.2}Ba_2Ca_2Cu_3O_{8+\delta}$ HTS bulk sample sintered at 1340 K for 10 min using the high gas pressure method.

appear either as rectangular, plate-like grains with dimensions ranging from 10 to 20 μm, or as oval grains of about 5–20 μm long and ca. 0.5–3 μm thick (Fig. 6(a)). The well-crystallized superconducting grains of the compact sample are oriented (Fig. 6(b)).

A semiquantitative elemental EDX analysis performed on the superconducting plate-like crystals yields an average Hg:Pb:Ba:Ca:Cu ratio of about 0.78:0.24:2.0:1.84:2.67, in approximate agreement with the overall composition of the superconductor (Fig. 7). The determined average content of Ca and Cu, which is smaller than that in the case of the stoichiometric (Hg,Pb)-1223 phase, is probably due to the coexistence of a small amount of intergrowth of a (Hg-1212 + Hg-1223)-type phase, as observed for the Hg-1223 sample investigated by means of transmission electron microscopy [43].

The following secondary phases are identified by means of EDX point analysis on the selected area of the superconducting sample: $BaCuO_2$, $CaHgO_2$, $BaPbO_3$, CuO, and $CaCu_2O_3$. $BaCuO_2$ is present in the form of well-separated crystallized grains with diameters ranging from 3 to 5 μm, as shown in Fig. 8(a). Small

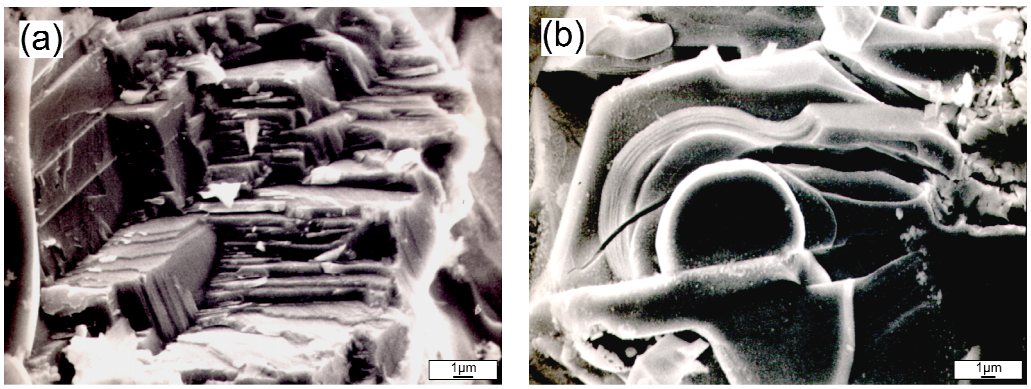

Fig. 6 SEM microphotographs of a fractured section of $Hg_{0.8}Pb_{0.2}Ba_2Ca_2Cu_3O_{8+\delta}$ HTS bulk sample sintered at 1340 K for 10 min using the high gas pressure method.

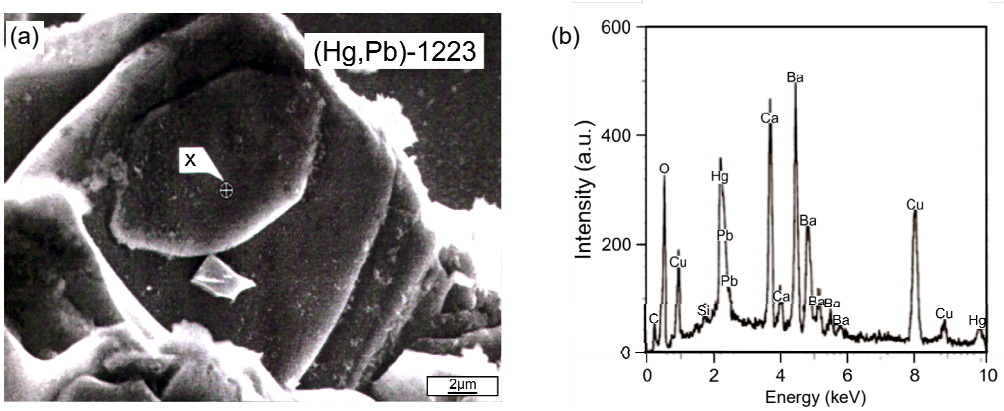

Fig. 7 (a) SEM microphotograph of a fractured section of $Hg_{0.8}Pb_{0.2}Ba_2Ca_2Cu_3O_{8+\delta}$ HTS bulk sample sintered at 1340 K for 10 min using the high gas pressure method and (b) EDX point analysis spectrum of point x.

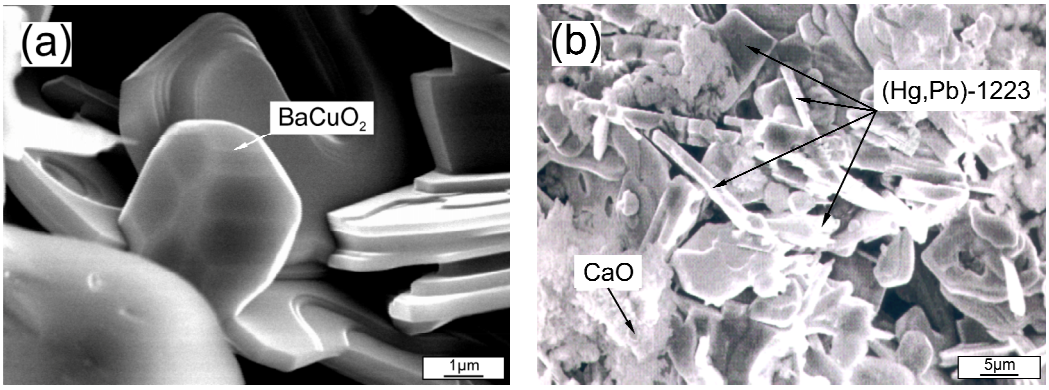

Fig. 8 SEM microphotographs of secondary phases of (a) $BaCuO_2$ and (b) CaO in $Hg_{0.8}Pb_{0.2}Ba_2Ca_2Cu_3O_{8+\delta}$ HTS bulk sample.

amounts of CaO particles with mushroom-like appearance and diameters between 2 and 10 μm are identified. The morphology of these particles is presented in Fig. 8(b). On the surface of HTS grains, the presence of very fine particles of a phase that most likely contains $CaHgO_2$ is observed; the latter phase could clearly be identified via XRD (Fig. 5).

Figure 9 shows these precipitates, which measure from 0.2 to 0.6 μm, making EDX analysis difficult, since the size of these particles is smaller than the spatial resolution. A similar morphological structure with the characteristic precipitates of $CaHgO_2$ particles on the grains of the HTS phase, but in a considerably greater amount than in the studied sample, has also been observed in the $HgPb_{0.4}Ba_2Ca_2Cu_3O_{8+\delta}$ superconductor prepared using a mixed oxide technique and solid-state reactions [44]. The $BaPbO_3$ and CuO phases are also detected in the analyzed sample.

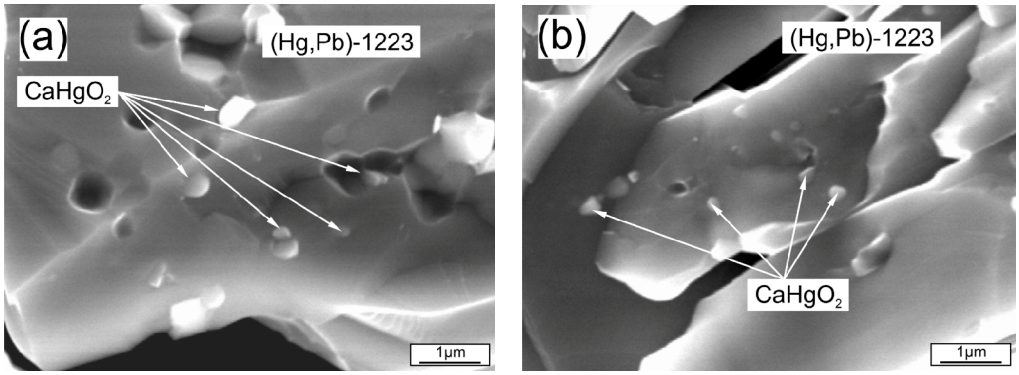

Fig. 9 SEM microphotographs of $CaHgO_2$ secondary phase formed on (Hg,Pb)-1223 superconductor grains.

Figure 10 shows the morphology of $BaPbO_3$ (Fig. 10(a)) and CuO (Fig. 10(b)) particles and the EDX point analysis spectra of these phases. In terms of dimensions, the particles of the former phase range from 1 to 1.5 μm, while the particles of the latter phase have a diameter of ca. 2 μm.

Figure 11 shows the temperature dependence of the AC susceptibility of the dispersive part χ' and the absorptive part χ'' for the $Hg_{0.8}Pb_{0.2}Ba_2Ca_2Cu_3O_{8+\delta}$ superconducting bulk sample. From the dependence curve $\chi'=f(T)$, it follows that this sample exhibits a double transition into the diamagnetic stage at temperatures of 129.2 and 123.4 K in a transition width of $\Delta T_c = 6.5$ K, and that it attains the susceptibility value of $\chi' = -7.5\times10^{-2}$ cm^3/g at 80 K [45]. These critical temperatures are slightly lower than those reported in the literature for the same system [46,47]. The second, slightly broader transition occurs due to the presence of the non-superconducting secondary phases within the microstructure of $(Hg,Pb)Ba_2Ca_2Cu_3O_{8+\delta}$, as observed

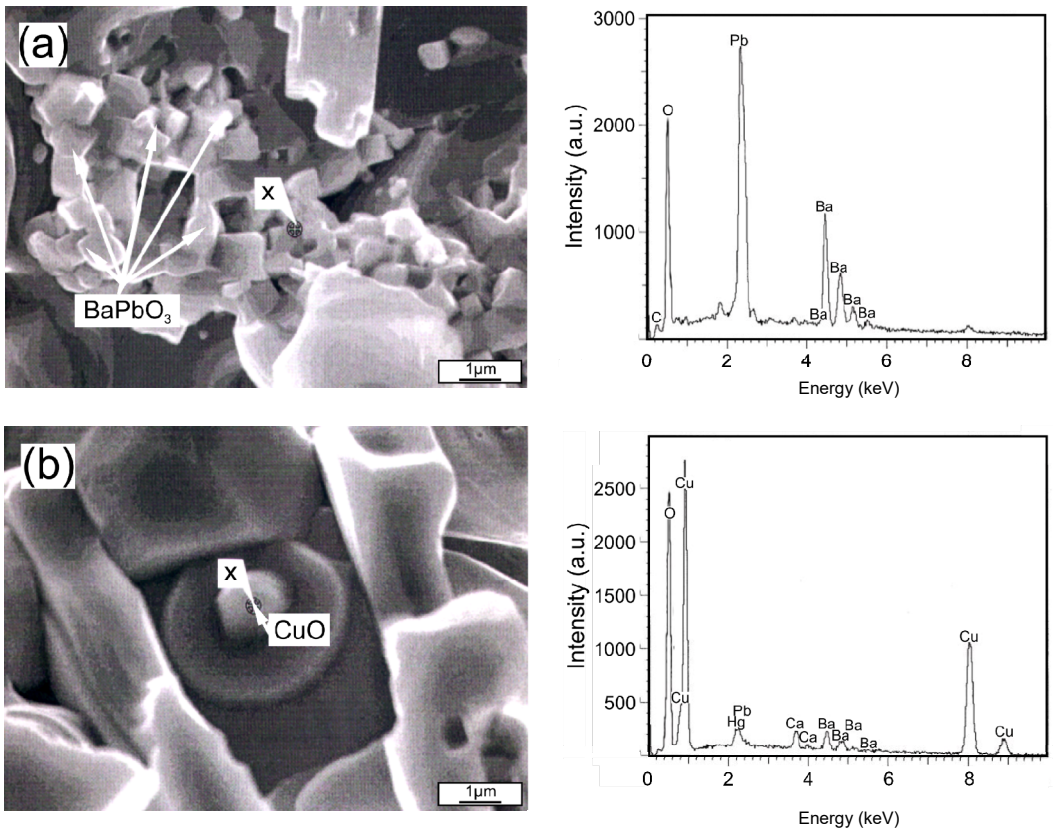

Fig. 10 SEM microphotographs of secondary phases of (a) $BaPbO_3$ and (b) CuO in $Hg_{0.8}Pb_{0.2}Ba_2Ca_2Cu_3O_{8+\delta}$ HTS bulk sample and EDX point analysis spectra of point x.

using XRD and SEM–EDX analyses. Moreover, this range of phase transition (ΔT_c) combined with the value of AC susceptibility (χ'_{80K}) might also be attributed to the porosity of the sample. The total porosity of the sample is ca. 17%. From the course of the dependence $\chi'' = f(T)$ shown in Fig. 11, it follows that the energy absorption of a variable magnetic field occurs in the temperature range of 117–130 K, with the maximum absorption value 7.0 cm^3/g at 125 K. This dependence indicates that the absorbed energy destroys a high number of intergranular links, which definitely confirms their narrow thickness distribution and the size distribution of microregions in intergranular links; these links contain a small amount of incompletely reacted spurious phases, allowing the material to obtain a sufficiently high critical current density. This is confirmed by the values of intragranular critical current densities for the $Hg_{0.8}Pb_{0.2}Ba_2Ca_2Cu_3O_{8+\delta}$ superconducting bulk sample as a function of the induction of the magnetic field, measured at 4 and 20 K; the results of these measurements are presented in Fig. 12. As can be seen in this plot, the critical current density, J_c, is strongly dependent on the measurement temperature and magnetic field induction. This is particularly evident at 20 K. The critical current density at 20 K and 1 T is approximately 26 A/mm^2, whereas at 4 K and 1 T it is equal to 155 A/mm^2. It is worth mentioning that for low values of the induction of the magnetic field, the increase in critical current entails the possibility of applying the superconductor investigated in the present paper to manufacture electrical cables. At 20 K, an electrical cable produced using the

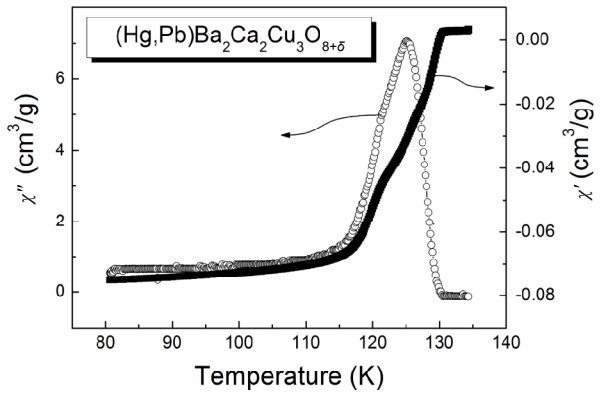

Fig. 11 Temperature dependence of AC susceptibility of dispersive part χ' and absorptive part χ'' of $Hg_{0.8}Pb_{0.2}Ba_2Ca_2Cu_3O_{8+\delta}$ HTS bulk sample sintered at 1340 K for 10 min using the high gas pressure method.

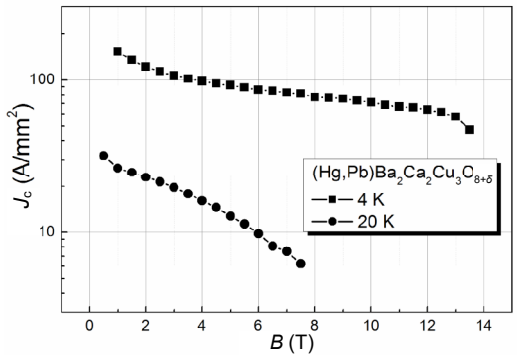

Fig. 12 The dependence of the critical current density of the $Hg_{0.8}Pb_{0.2}Ba_2Ca_2Cu_3O_{8+\delta}$ HTS bulk sample on the induction of the magnetic field at 4 and 20 K.

$Hg_{0.8}Pb_{0.2}Ba_2Ca_2Cu_3O_{8+\delta}$ material would exhibit a critical current density similar to that of magnesium diboride, which hints at the possibility of replacing MgB_2 with (Hg,Pb)-1223 at the temperature of liquid neon.

4 Conclusions

Fine, homogenous Hg-free precursor powders of $Ba_2Ca_2Cu_3O_x$ with desired chemical and phase compositions were successfully obtained using EDTA gel process based on the complexation of metal cations by EDTA, which forms strong, soluble chelate complexes with the aforementioned metal ions. A polycrystalline sample of the $Hg_{0.8}Pb_{0.2}Ba_2Ca_2Cu_3O_{8+\delta}$ superconductor was obtained via the thermal treatment of Hg-free precursor powders in the mercury vapor environment using the high gas pressure method. The sample was composed predominantly of the (Hg,Pb)-1223 phase (T_c = 129.2 K, ΔT_c = 6.5 K) in the form of plate-like crystallites or oval grains with the preferred orientation. The critical current density for the $Hg_{0.8}Pb_{0.2}Ba_2Ca_2Cu_3O_{8+\delta}$ sample at 20 K and 1 T was approximately 26 A/mm^2, while at 4 K and 1 T it increased to 155 A/mm^2. Various secondary phases with low volume fractions of $BaCuO_2$, CaO, $CaHgO_2$, CuO, and $BaPbO_3$ within the microstructure of the $Hg_{0.8}Pb_{0.2}Ba_2Ca_2Cu_3O_{8+\delta}$ bulk sample were identified by means of SEM–EDX. The high volume fraction of the (Hg,Pb)-1223 phase (89.1%) in the $Hg_{0.8}Pb_{0.2}Ba_2Ca_2Cu_3O_{8+\delta}$ sample may be associated with the determined low value of the average copper valence equal to 2.11 in the $Ba_2Ca_2Cu_3O_x$ precursor.

Acknowledgements

The authors would like to express their gratitude to Mrs. B. Trybalska from the Faculty of Materials Science and Ceramics, AGH University of Science and Technology, Krakow, Poland, for her assistance in SEM–EDX observations.

References

[1] Putilin SN, Antipov EV, Chmaissem O, *et al*. Superconductivity at 94 K in $HgBa_2Cu0_{4+\delta}$. *Nature* 1993, **362**: 226–228.

[2] Putilin SN, Antipov EV, Marezio M. Superconductivity above 120 K in $HgBa_2Cu_2O_{6+\delta}$. *Physica C* 1993, **212**: 266–270.

[3] Meng RL, Beauvais L, Zhang XN, *et al*. Synthesis of the high-temperature superconductors $HgBa_2Cu_2O_{6+\delta}$ and $HgBa_2Ca_2Cu_3O_{8+\delta}$. *Physica C* 1993, **216**: 21–28.

[4] Schilling A, Cantoni M, Guo JD, *et al*. Superconductivity above 130 K in the Hg–Ba–Ca–Cu–O system. *Nature* 1993, **363**: 56–58.

[5] Schilling A, Jeandupeux O, Guo JD, *et al*. Magnetization and resistivity study on the 130 K superconductor in the Hg–Ba–Ca–Cu–O system. *Physica C* 1993, **216**: 6–11.

[6] Chu CW, Gao L, Chen F, *et al*. Superconductivity above 150 K in $HgBa_2Ca_2Cu_3O_{8+\delta}$ at high pressures. *Nature* 1993, **365**: 323–325.

[7] Schilling A, Jeandupeux O, Büchi S, *et al*. Physical properties of $HgBa_2Ca_2Cu_3O_8$ with $T_c \approx 133$ K. *Physica C* 1994, **235–240**: 229–232.

[8] Wagner JL, Radaelli PG, Hinks DG, *et al*. Structure and superconductivity of $HgBa_2CuO_{4+\delta}$. *Physica C* 1993, **210**: 447–454.

[9] Lin CT, Yan Y, Peters K, *et al*. Flux growth $Hg_{1-x}Re_xBa_2Ca_{n-1}Cu_nO_{2n+2+\delta}$ single crystals by self-atmosphere. *Physica C* 1998, **300**: 141–150.

[10] Sin A, Cunha AG, Calleja A, *et al*. Formation and stability of $HgCaO_2$, a competing phase in the synthesis of $Hg_{1-x}Re_xBa_2Ca_2Cu_3O_{8+\delta}$ superconductor. *Physica C* 1998, **306**: 34–46.

[11] Kandyel E, Elsabawy KM. New 1201-Type (Hg,Se)-superconducting cuprate grown by sol–gel and sealed quartz tube synthesis. *Physica C* 2008, **468**: 2322–2327.

[12] Przybylski K, Morawski A, Łada T, *et al*. Synthesis and properties of $(Hg_{1-x}Re_x)Ba_2Ca_2Cu_3O_{8+\delta}$ HTS single crystals and films obtained by high-pressure gas method. *Physica C* 2000, **341–348**: 543–544.

[13] Isawa K, Tokiwa-Yamamoto A, Itoh M, *et al*. Encapsulation method for the synthesis of nearly single-phase superconducting $HgBa_2Ca_2Cu_3O_{8+\delta}$ with $T_c \approx 135$ K. *Physica C* 1994, **222**: 33–37.

[14] Shao HM, Shen LJ, Shen JC, *et al*. Synthesis of single-phase $HgBa_2Ca_2Cu_3O_{8+\delta}$ superconductor. *Physica C* 1994, **232**: 5–9.

[15] Tokiwa-Yamamoto A, Isawa K, Itoh M, *et al*. Composition, crystal structure and superconducting properties of Hg–Ba–Cu–O and Hg–Ba–Ca–Cu–O superconductors. *Physica C* 1993, **216**: 250–256.

[16] Shao HM, Lam CC, Fung PC, *et al*. The synthesis and characterization of $HgBa_2Ca_2Cu_3O_{8+\delta}$ superconductors with substitution of Hg by Pb. *Physica C* 1995, **246**: 207–215.

[17] Lee S, Shlyakhtin OA, Mun M-O, *et al*. A freeze-drying approach to the preparation of $HgBa_2Ca_2Cu_3O_{8+x}$ superconductor. *Supercond Sci Technol* 1995, **8**: 60–65.

[18] Mendonça TM, Tavares PB, Correia JG, *et al*. The urea combustion method in the preparation of precursors for high-T_C single phase $HgBa_2Ca_2Cu_3O_{8+\delta}$ superconductors. *Physica C* 2011, **471**: 1643–1646.

[19] Isawa K, Tokiwa-Yamamoto A, Itoh M, *et al*. The effect of Pb doping in $HgBa_2Ca_2Cu_3O_{8+\delta}$ superconductor. *Physica C* 1993, **217**: 11–15.

[20] Kirschner I, Laiho R, Lukács P, *et al*. Effect of preparation on Hg–Ba–Ca–Cu–O superconductors. *Z Phys B Con Mat* 1996, **99**: 501–506.

[21] Sin A, Odier P, Weiss F, *et al*. Synthesis of (Hg,Re-1223) by sol–gel technique. *Physica C* 2000, **341–348**: 2459–2460.

[22] Antipov EV, Loureiro SM, Chaillout C, *et al*. The synthesis and characterization of the $HgBa_2Ca_2Cu_3O_{8+\delta}$ and $HgBa_2Ca_3Cu_4O_{10+\delta}$ phases. *Physica C* 1993, **215**: 1–10.

[23] Lin QM, He ZH, Sun YY, *et al*. Precursor effects on $HgBa_2Ca_2Cu_3O_8$ formation under high pressure. *Physica C* 1995, **254**: 207–212.

[24] Loureiro SM, Stott C, Philip L, *et al*. The importance of the precursor in high-pressure synthesis of Hg-based superconductors. *Physica C* 1996, **272**: 94–100.

[25] Kareiva A, Barkauskas J, Mathur S. Oxygen content and superconducting properties of Hg-based superconductors synthesized by sol–gel method. *J Phys Chem Solids* 2000, **61**: 789–797.

[26] Bryntse I, Kareiva A. Superconductivity in $HgBa_2Ca_2Cu_3O_{8+\delta}$ synthesized by different methods. *Mater Res Bull* 1995, **30**: 1207–1216.

[27] Przybylski K, Brylewski T. Synthesis of high-T_c (Bi,Pb)–Sr–Ca–Cu–O and Y–Ba–Cu–O superconductors by sol–gel technique. In Proceedings of Join Europe–USA Conferences on Superconductivity ICMAS-92, 1992: 67–72.

[28] Brylewski T, Przybylski K. Physicochemical properties of high-T_c (Bi,Pb)–Sr–Ca–Cu–O and Y–Ba–Cu–O superconductors prepared by sol–gel technique. *Appl Supercond* 1993, **1**: 737–744.

[29] Sin A, Cunha AG, Calleja A, *et al*. Influence of precursor oxygen stoichiometry on the formation of Hg, Re-1223 superconductors. *Supercond Sci Technol* 1999, **12**: 120–127.

[30] Morawski A, Łada T, Pachla W, *et al*. Crystal growth of $YBa_2Cu_4O_8$ superconducting single crystals under high oxygen pressure. In Proceedings of Join Europe–USA Conferences on Superconductivity ICMAS-91, 1991: 361–366.

[31] Przybylski K. Physicochemical properties of high-T_c materials—preparation and characterization of

Tl–Ba–Ca–Cu–O and Hg–Ba–Ca–Cu–O superconducting thick and thin films. In: *Textbook of the 4th International Summer School on High Temperature Superconductivity*. Vajda I, Szalay A, Porjesz T, *et al*. Eds. Eger, Hungary, 1998: 33–61.

[32] Morawski A, Łada T, Paszewin A, *et al*. High gas pressure for HTS single crystals and thin layer technology. *Supercond Sci Technol* 1998, **11**: 193–199.

[33] Nazzal AI, Lee VY, Engler EM, *et al*. New procedure for determination of $[Cu–O]^{+p}$ charge and oxygen content in high T_c copper oxide. *Physica C* 1988, **153–155**: 1367–1368.

[34] Bean CP. Magnetization of hard superconductors. *Phys Rev Lett* 1962, **8**: 250.

[35] Kakihana M. Invited review "sol–gel" preparation of high temperature superconducting oxides. *J Sol–Gel Sci Technol* 1996, **6**: 7–55.

[36] Sillèn LG, Martell AE. Stability constants of metal-ion complexes. Specical Publication No. 25. Chemical Society, London, 1971.

[37] Day RA Jr., Underwood AL. *Quantitative Analysis, Laboratory Manual*, 2nd edn. Englewood Cliffs, New Jersey, USA: Prentice-Hall, Inc., 1967.

[38] Van der Biest O, Kwarciak J, Dierickx D, *et al*. Ceramic superconductors synthesized by sol–gel methods. *Physica C* 1991, **190**: 119–121.

[39] Ringbom A. *Complexation in Analytical Chemistry: A Guide for the Critical Selection of Analytical Methods Based on Complexation Reactions*. New York: Interscience, 1963.

[40] Whiter JD, Roth RS. *Phase Diagrams for High-T_c Superconductors*. Westerville, Ohio, USA: Amer Ceramic Society, 1991.

[41] Rui Y, Ji HL, Shao HM, *et al*. Characterization of Hg–Ba–Ca–Cu–O 1223 superconductor. *Physica C* 1994, **231**: 243–248.

[42] Martin K, McCarthy G. JCPDS-International Center for Diffraction Data, No. 44-1481.

[43] Cantoni C, Schilling A, Nissen HU, *et al*. Characterisation of superconducting Hg–Ba–Ca–Cu–oxides: Structural and physical aspects. *Physica C* 1993, **215**: 11–18.

[44] Kellner K, Przybylski K, Gritzner G. Microstructure and phase composition of Hg-1223 bulk phase superconductors. *Physica C* 1998, **307**: 99–104.

[45] Przybylski K, Brylewski T, Morawski A, *et al*. $Ba_2Ca_2Cu_3O_x$ precursor effects on synthesis of $(Hg,Pb)Ba_2Ca_2Cu_3O_{8+\delta}$ superconductor. *J Therm Anal Calorim* 2001, **65**: 391–398.

[46] Armstrong AR, David WIF, Gameson I, *et al*. Crystal structure of $HgBa_2Ca_2Cu_3O_{8+\delta}$ at high pressure (to 8.5 GPa) determined by powder neutron diffraction. *Phys Rev B* 1995, **52**: 15551–15557.

[47] Abu-Aljarayesh I, Hamam YA, Said MR. Magnetization study of $HgBa_2Ca_2Cu_3O_{8+\delta}$ high-temperature superconductors. *Supercond Sci Technol* 1997, **10**: 290–297.